Eur. Phys. J. D **39**, 385–389 (2006)
DOI: 10.1140/epjd/e2006-00107-2

THE EUROPEAN PHYSICAL JOURNAL D

Studies on vibrational excitation differential cross-sections of low-energy electron scattering from N_2 molecule

W. Dai[1,a], W.G. Sun[1,b], H. Feng[2], and L. Shen[1]

[1] Institute of Atomic and Molecular Physics, Sichuan University, Chengdu 610065, P.R. China
[2] College of Physics, Sichuan University, Chengdu 610065, P.R. China

Received 19 January 2006 / Received in final form 26 March 2006
Published online 18 May 2006 –

Abstract. The vibrational excitation differential cross-sections (DCS) of low-energy electron-N_2 scattering are studied using vibrational close-coupling (VCC) method and vibrational scattering potentials which include static, exchange and polarization contributions. By including the contributions of 18 partial waves, 20 vibrational states, and 16 molecular symmetries (up to $\Lambda = 7$), the converged vibrational excitation ($0 \to 2$, $0 \to 3$, $0 \to 4$) DCS agree well with experimental results. Also obtained are converged vibrational ($1 \to 0$, $1 \to 1$, $1 \to 2$, $1 \to 3$) DCS, with the impact energies being those of the main resonant peaks (1.92 eV, 1.90 eV, 1.62 eV, 1.63 eV).

PACS. 34.80.Bm Elastic scattering of electrons by atoms and molecules

1 Introduction

Differential cross-sections show the characteristic structure and kinetic information of incident particles and target. N_2 is a typical small nonspherical molecule between two-electron molecule H_2 and other multi-electron molecules, it has long been a fertile field for investigations of low-energy electron scattering. Studies on this field are important to astrophysics, meteoric physics, solid physics, chemical physics, gas-discharge devices, and the modeling of laser kinetics [1–5].

There have been many important theoretical and experimental studies on electron-N_2 collisions. The representative theories are: the Schwinger variational method of Mckoy and Huo [6,7], the hybrid theory of Weatherford and Temkin [8], the R-matrix method of Burke and Gillan [9], the boomerang model of Dube and Herzenberg [10], and the close-coupling method of Morrison and Saha [11]. In 1995, Weiguo Sun, Morrison, Buckman, and coworkers [12] reported their comprehensive studies on the $0 \to 0$ and $0 \to 1$ vibrational cross-sections of electron-N_2 scattering using vibrational close-coupling (VCC) method theoretically, and cross beam method and time of flight (TOF) method experimentally. Excellent agreement between their theoretical and experimental results has been attained, and an effective protocol has been suggested to systematically compare theoretical and experimental differential cross-sections (DCS) of electron scattering form molecules in resonant region. Recently, Hao Feng, Weiguo Sun and Morrison [13] proposed a model correlation-polarization potential for vibrational excitation in electron-molecule scattering, based on the work of Bouferguene [14]. They regard the scattering electron as a spherical charge density that decays with radial distance from r_e.

Vibrational differential cross-sections play an important role in the field of discharge physics studies [15,16]. Allan measured the vibrational DCS of electron-N_2 scattering using cross beam method [6]. His data have about 30% error and have notable difference with Wong's experiment [10], Error from Sweeney's experiment [17] is 23%. Therefore, it is necessary to do further study on vibrational differential cross-sections.

Most of the previous studies on electron-N_2 scattering only demonstrated target (N_2) in ground state. Up to now, we haven't found any experimental report about differential cross-sections when the target (N_2) in excited state. In this paper, some results of our studies on the differential cross-sections ($1 \to 0$, $1 \to 1$, $1 \to 2$, $1 \to 3$) are reported.

2 Theory

From the Schrödinger equation, using the fixed nuclei orientation (FNO) approximation, denoting the entrance-channel by the subscript 0 and exit-channel by the subscript v, the integral-differential equation of vibrational

[a] e-mail: dai13545679420@126.com
[b] *Permanent address*: Institute of Atomic and Molecular Physics, Sichuan University, Chengdu 610065, P.R. China.

close-coupling can be expressed as follow [18]

$$\left[\frac{1}{2}\frac{d^2}{dr^2} - \frac{l(l+1)}{2r^2} - V^{\Lambda}_{vl,vl}(r) + \frac{1}{2}k_v^2\right] u^{\Lambda}_{vl,v_0l_0}(r) = \sum_{v',l'\neq v,l} \left[V^{\Lambda}_{vl,v'l'}(r) u^{\Lambda}_{v'l',v_0l_0}(r)\right] \quad (1)$$

where

$$\frac{1}{2}k_v^2 = \frac{1}{2}k_0^2 - (\varepsilon_v - \varepsilon_0) \quad (2)$$

here $k_0^2/2$ is the entrance-channel energy of incident electron, $k_v^2/2$ is the exit-channel energy of it, ε_v is the energy of the vth vibrational state, ε_0 is the energy of ground state.

The matrix elements of the total interaction potential energy can be expressed as

$$V^{\Lambda}_{vl,v'l'}(r) = \langle v, l; \Lambda | V_{tot}(r,R) | v', l'; \Lambda \rangle_{R,r}\,. \quad (3)$$

In this paper, total interaction potential $V_{tot}(r,R)$ contains three components: static potential, exchange potential and correlation-polarization terms [19,20], it is expanded in terms of Legendre polynomial

$$V_{tot}(r,R) = V_{st} + V_{ex} + V_{cp} = {\sum_{\lambda=0}^{\infty}}' v_\lambda(r,R) P_\lambda(\cos\theta_e) \quad (4)$$

where the prime signifies that for homonuclear targets this sum includes only even values of λ, $v_\lambda(r,R)$ is Legendre projection. The static term V_{st} arises form Coulomb interactions between the projectile and the constituents of the target. The exchange term V_{ex} rises from the antisymmetrization requirement of the electron-molecule wavefunction. The correlation-polarization term V_{cp} arises from many-body correlation and induced polarization effects. These potentials are nonspherical. The exchange and the polarization potentials are nonlocal in nature, and they are calculated using local approximation in this study. The tuned free electron gas exchange (TFEGE) model [12] is used for the exchange potential. The basic physics of the TFEGE is that all electrons move in an average potential, and the TFEGE is calculated from the charge density obtained using quantum mechanical ab initio method. The better than adiabatic dipole (BTAD) potential is used for the correlation-polarization potential [12].

The angular integration in the potential matrix elements (3) is now easily performed using the Gaunt formula

$$V^{\Lambda}_{vl,v'l'}(r) = \sum_{\lambda=0}^{\lambda_{\max}} g_\lambda(ll';\Lambda)\omega^{\lambda}_{v,v'}(r) \quad (5)$$

where the angular coupling coefficient $g_\lambda(ll';\Lambda)$ and the radial vibrational coupling potential $\omega^{\lambda}_{v,v'}(r)$ are

$$g_\lambda(ll';\Lambda) = \left[\frac{2l'+1}{2l+1}\right]^{1/2} C(l'\lambda l;\Lambda 0) C(l'\lambda l;00) \quad (6)$$

$$\omega^{\lambda}_{v,v'}(r) \equiv \langle \varphi_v | v_\lambda | \varphi_{v'} \rangle = \int_0^\infty \varphi_v^*(R) v_\lambda(r,R) \varphi_{v'}(R) dR. \quad (7)$$

According to boundary conditions, we can get scattering matrix K from (1),

$$K^{\Lambda}_{v,v_0} = -\frac{2}{\sqrt{k_v k_0}} \sum_{v'} \int_0^\infty \hat{j}_l(k_v r) V^{\Lambda}_{v,v'}(r) u^{\Lambda}_{v,v'}(r) dr \quad (8)$$

matrix S, matrix T, matrix K have the following relation,

$$S^{\Lambda} = 1 + 2iT^{\Lambda} = (1 + iK^{\Lambda})(1 - iK^{\Lambda})^{-1} \quad (9)$$

while the swing of scattering can be expressed by matrix T as follow,

$$f_{v,v_0}(\hat{r}) = \frac{4\pi}{\sqrt{k_v k_0}} \times \sum_{l=0}^{l_{\max}} \sum_{l_0=0}^{l_{\max}} \sum_{\Lambda=-l}^{l} i^{l_0-l} Y_l^{\Lambda}(\hat{k}_v) T^{\Lambda}_{vl,v_0l_0} Y_{l_0}^{\Lambda *}(\hat{k}_0) \quad (10)$$

then the DCS is expanded in terms of Legendre polynomial in the laboratory frame (LF) can be expressed as follow,

$$\frac{d\sigma}{d\Omega}|_{v_0\to v} \equiv \frac{1}{4k_0^2} \sum_{L=0}^{L_{\max}} B_L(v_0 \to v) P_L(\cos\theta') \quad (11)$$

where θ' is the LF scattering angle, k_0 is wave number of incident channel, and $B_L(v_0 \to v)$ is the expansion coefficient,

$$B_L(v_0 \to v) = \sum_{\Lambda\bar{\Lambda}} \sum_{l\bar{l}} \sum_{l_0\bar{l}_0} d_L(ll_0, \bar{l}\bar{l}_0; \Lambda\bar{\Lambda}) T^{\Lambda}_{vl,v_0l_0} T^{\bar{\Lambda}^*}_{v\bar{l},v_0\bar{l}_0} \quad (12)$$

T^{Λ}_{vl,v_0l_0} is matrix element T of vibrational scattering, $d_L(ll_0, \bar{l}\bar{l}_0; \Lambda\bar{\Lambda})$ is angular momentum coupling coefficient,

$$d_L(ll_0, \bar{l}\bar{l}_0; \Lambda\bar{\Lambda}) = i^{l_0-l-\bar{l}_0} \frac{1}{2L+1} \big[(2l+1)(2\bar{l}+1) \times (2l_0+1)(2\bar{l}_0+1)\big]^{1/2} C(l\bar{l}L;0,0) C(l\bar{l}L;\Lambda,-\bar{\Lambda}) \quad (13)$$

where C is Clebsch-Gordan coefficients.

3 Computational method

All fundamental vibrational scattering information is included in equation (1). Solving this equation, the first step is converting it into the second type Volterra equation, and then calculating it numerically using the Green's function method of integral equation from the origin to the asymptotic region of the scattering system.

The dimension of the radial wavefunctions matrix of the vibrational coupling equation (1) is "$nv \times nl$" when "nv" vibrational wavefunctions and "nl" partial waves are specified. More partial waves is required to converge the numerical radial scattering wavefunctions $u^{\Lambda}_{vl,v_0l_0}(r)$ near the target (small r) due to strong centrifugal potential and nonspherical static potential, while less partial waves may converge the calculation in the asymptotic scattering (large r) region. The number of partial

Table 1. Vibrational differential cross-sections (in square Bohr) of low-energy electron scattering from N_2, energies are chosen to represent the peaks of oscillations in cross-sections.

Angle	2.10 eV			1.92 eV	1.90 eV	1.62 eV	1.63 eV
(deg.)	$(0 \to 2)$	$(0 \to 3)$	$(0 \to 4)$	$(1 \to 0)$	$(1 \to 1)$	$(1 \to 2)$	$(1 \to 3)$
0	1.1551	1.1675	0.4908	5.7749	7.7754	4.5371	1.7899
5	1.1345	1.1467	0.4821	5.6731	7.7649	4.4562	1.7578
10	1.0744	1.0861	0.4566	5.3769	7.7437	4.2211	1.6648
15	0.9808	0.9915	0.4168	4.9126	7.7157	3.8537	1.5198
20	0.8626	0.8721	0.3666	4.3225	7.6407	3.3882	1.3365
25	0.7308	0.7388	0.3106	3.6607	7.4484	2.8679	1.1322
30	0.5973	0.6038	0.2538	2.9873	7.0969	2.3402	0.9252
35	0.4735	0.4785	0.2011	2.3616	6.6103	1.8515	0.7332
40	0.3693	0.3729	0.1567	1.8343	6.0620	1.4413	0.5714
45	0.2917	0.2943	0.1237	1.4418	5.5289	1.1382	0.4509
50	0.2443	0.2462	0.1035	1.2028	5.0568	0.9566	0.3774
55	0.2274	0.2289	0.0963	1.1174	4.6526	0.8965	0.3510
60	0.2375	0.2389	0.1006	1.1684	4.2994	0.9438	0.3664
65	0.2681	0.2697	0.1136	1.3244	3.9787	1.0733	0.4138
70	0.3110	0.3130	0.1318	1.5437	3.6841	1.2515	0.4802
75	0.3569	0.3594	0.1514	1.7804	3.4200	1.4418	0.5513
80	0.3971	0.4002	0.1685	1.9899	3.1898	1.6087	0.6137
85	0.4243	0.4278	0.1802	2.1351	2.9885	1.7229	0.6559
90	0.4337	0.4376	0.1843	2.1915	2.8039	1.7651	0.6706
95	0.4238	0.4279	0.1801	2.1499	2.6261	1.7283	0.6554
100	0.3962	0.4002	0.1685	2.0178	2.4562	1.6190	0.6127
105	0.3557	0.3595	0.1513	1.8184	2.3092	1.4558	0.5501
110	0.3096	0.3131	0.1317	1.5876	2.2086	1.2677	0.4788
115	0.2668	0.2698	0.1135	1.3691	2.1786	1.0899	0.4124
120	0.2364	0.2390	0.1005	1.2093	2.2374	0.9591	0.3654
125	0.2268	0.2290	0.0963	1.1501	2.3953	0.9090	0.3505
130	0.2444	0.2462	0.1036	1.2237	2.6553	0.9652	0.3775
135	0.2925	0.2942	0.1239	1.4476	3.0151	1.1417	0.4519
140	0.3711	0.3728	0.1570	1.8218	3.4656	1.4384	0.5735
145	0.4763	0.4783	0.2015	2.3281	3.9893	1.8410	0.7364
150	0.6011	0.6035	0.2543	2.9319	4.5586	2.3216	0.9295
155	0.7356	0.7385	0.3112	3.5853	5.1370	2.8418	1.1377
160	0.8683	0.8717	0.3674	4.2318	5.6831	3.3567	1.3430
165	0.9872	0.9911	0.4177	4.8125	6.1558	3.8191	1.5270
170	1.0812	1.0855	0.4575	5.2728	6.5198	4.1856	1.6726
175	1.1415	1.1461	0.4830	5.5683	6.7489	4.4209	1.7659
180	1.1623	1.1670	0.4918	5.6701	6.8271	4.5020	1.7981

waves in equation (1) is reduced to $nl' = 3$ from $nl = 18$ at $r = 6.0a_0$, which greatly reduces the computational efforts used to propagate the numerical scattering functions from $r = 6.0a_0$ to the maximum scattering distance $r_{\max} = 85.0a_0$; for $r_e > 85.0a_0$, we used Born completion to evaluate additional higher-order elements of the K matrix required to converge the differential cross-sections.

The contributions of high-order angular momentum to scattering quantities are mainly affected by the long range correlation-polarization potentials which, although weak, are important for long range scattering.

There is a twofold summation over molecular symmetries Λ in equation (12). The close-coupling K matrix and the Born K matrix are calculated respectively according to the above discussions for Σ and $\Pi(\Lambda = 0, 1)$ symmetries of N_2. Although the K matrices of high-order symmetries of N_2 may be neglected for integral cross-sections, their contributions to the DCS of small angle scattering are important. The scattering matrices of the first four symmetries $(\sigma_g, \sigma_u, \pi_g, \pi_u)$ are calculated by VCC method, and those of other twelve "Born symmetries" by Born coupling method.

4 Results and discussion

Using the improved method of vibrational close-coupling, DCS converge better than before. The converged vibrational excitation DCS are obtained when using 20 Morse vibrational states, 18 partial waves, and 16 molecular symmetries. The scattering matrices of the first four symmetries $(\sigma_g, \sigma_u, \pi_g, \pi_u)$ are calculated by VCC method, and those of other twelve "Born symmetries" by Born coupling method. In our previous studies, we used $nl = 11$ at the short range, it was not convergent enough for $0 \to 2, 0 \to 3$

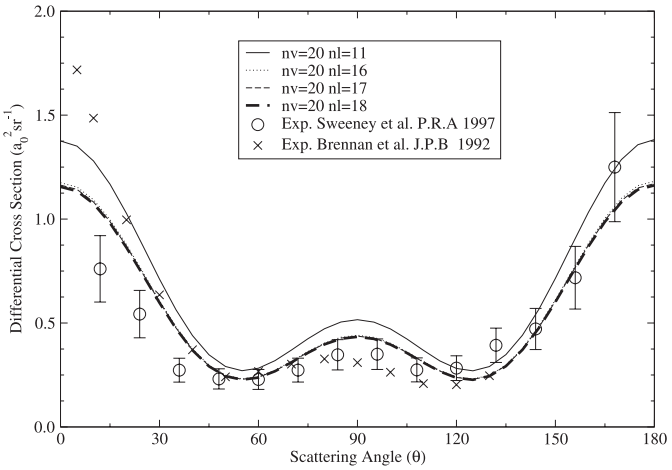

Fig. 1. Vibrational excitation ($0 \rightarrow 2$) differential cross-sections of low-energy (2.10 eV) electron scattering from N_2 molecule.

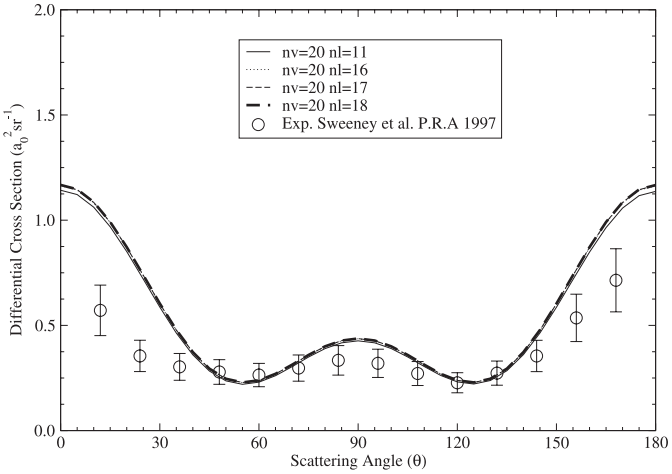

Fig. 2. Vibrational excitation ($0 \rightarrow 3$) differential cross-sections of low-energy (2.10 eV) electron scattering from N_2 molecule.

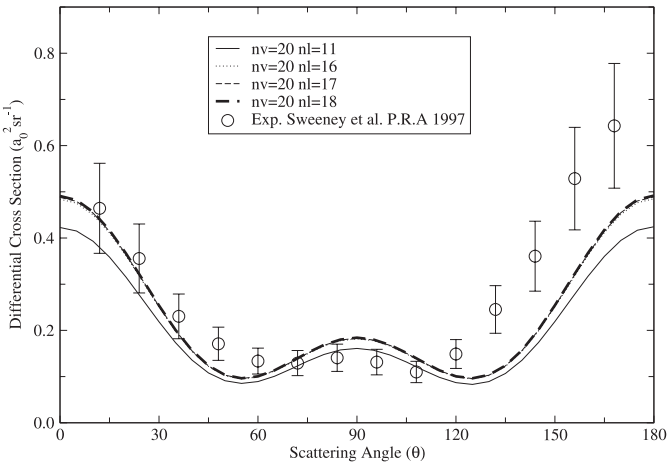

Fig. 3. Vibrational excitation ($0 \rightarrow 4$) differential cross-sections of low-energy (2.10 eV) electron scattering from N_2 molecule.

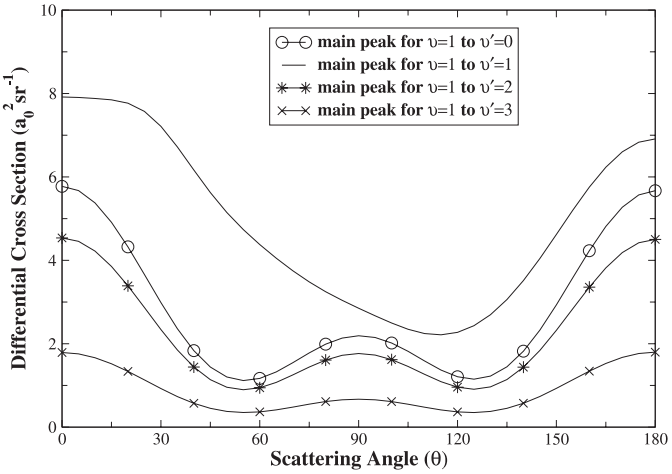

Fig. 4. Vibrational ($1 \rightarrow 0, 1, 2, 3$) differential cross-sections of low-energy electron scattering from N_2 molecule. The impact energies are those of the main resonant peaks (1.92 eV, 1.90 eV, 1.62 eV, 1.63 eV).

and $0 \rightarrow 4$ vibrational excitations (see Figs. 1, 2 and 3), here we enlarge the scattering channels and use $nl = 18$.

We compare our 2.1 eV impact DCS with those measured by Sweeney et al. [17] and Brennan et al. [21], the impact energy 2.10 eV is the second resonant peak of elastic scattering. Figure 1 shows the vibrational excitation DCS of $0 \rightarrow 2$, the theoretical DCS of this study agrees well with experimental data from Sweeney et al. and Brennan et al. when scattering angle is higher than 45°, from 0° to 45°, Sweeney's results have notable difference from Brennan's experiment, remarkably, when the scattering angle is small, the experiments of cross beam have great challenge to measure accurately, Brennan's is high, Sweeney's is low, and ours is in the middle. To so remarkable difference between two experiments, it deserves experimenter to explore a new way to measure DCS in small angle. Displayed in Figure 2 are the DCS of $0 \rightarrow 3$, our results agree with Sweeney's experiment between 45° to 135°, in areas of small and large angle, our DCS are greater than those of Sweeney's. Figure 3 compares resonant DCS of $0 \rightarrow 4$ from our calculations with data from Sweeney. Contrary to $0 \rightarrow 3$, at angles above 105°, our results are lower than those of experiment, and agree well in other areas.

The vibrational DCS of $\upsilon = 1 \rightarrow \upsilon' = 0, 1, 2, 3$ are presented in Figure 4, With the impact energies being those of the main resonant peaks-approximately 1.92 eV, 1.90 eV, 1.62 eV, 1.63 eV (1.92 eV is energy of the main resonant peak for $\upsilon = 1 \rightarrow \upsilon' = 0$, 1.90 eV is energy of the main resonant peak for $\upsilon = 1 \rightarrow \upsilon = 1$, 1.62 eV is energy of the main resonant peak for $\upsilon = 1 \rightarrow \upsilon' = 2$, 1.63 eV is energy of the main resonant peak for $\upsilon = 1 \rightarrow \upsilon' = 3$). We obtain converged vibrational excitation DCS when the target is in excited state, which is difficult to get by experiment. The DCS of $\upsilon = 1 \rightarrow \upsilon' = 1$ are bigger than others, though they are not in the same impact energy, but all energies

are in main peaks, they represent the largest probability of scattering, which agree with principle of Franck-Condom. That is, the probability of perpendicularity transition is the greatest, usually the DCS of elastic scattering are bigger than those of inelastic scattering.

Generally, among all methods of studies on e–N_2 scattering, vibrational close-coupling (VCC) method is better than others at the aspect of precision. It takes into account the coupling among different vibrational states during the process of scattering, and also describes the vibrational process accurately. However the dipole polarization approximation on polarization potential, and the local approximation on nonlocal exchange and polarization potentials both influence the results by a certain extent. At the same time, static potential, exchange potential and correlation-polarization are sensitive to wavefunction of molecular system. Though it is suitable to describe molecular system of closed shell by single configuration Hartree-Fock wavefunction, yet we had better adopt comprehensive wavefunction to reflect fine resonance structure. On the other hand, error from Christopher J. Sweeney's experiment is also up to 23%. All of those enlarge the difference between theory and experiment. Therefore, it is necessary to do further study on e–N_2 scattering.

The authors are grateful to Michael A. Morrison. This project is supported by the Chinese National Natural Science Foundation (Grant Number: 10474068) and the Science Foundation of the Chinese Educational Ministry.

References

1. X.M. Liu et al., Am. Astron. Soc. **623**, 1 (2005)
2. D.C. Tyte, Adv. Quant. Electron **1**, 129 (1970)
3. R.A. Haas, Phys. Rev. A **8**, 1017 (1973)
4. G.J. Schulz, *Principles of Laser Plasmas*, edited by G. Bekite (Wiley, New York, 1976), Chap. 2
5. A.V. Phelps, *Electron-Molecule Scattering*, edited by S.C. Brown (Wiley-Interscience, New York, 1979), Chap. 2
6. W.M. Huo et al., Progr. Astron. Aeron. **103**, 152 (1986)
7. W.M. Huo et al., Phys. Rev. A **36**, 1642 (1987)
8. C.A. Weatherford, A. Temkin, Phys. Rev. A **49**, 2580 (1994)
9. C.J. Gillan et al., J. Phys. B: At. Mol. Phys. **20**, 4858 (1987)
10. L. Dube, A. Herzenberg, Phys. Rev. A **20**, 194 (1979)
11. M.A. Morrison, B.C. Saha, Phys. Rev. A **34**, 2796 (1986)
12. W.G. Sun et al., Phys. Rev. A **52**, 1229 (1995)
13. H. Feng, W.G. Sun, M.A. Morrision, Phys. Rev. A **68**, 062709 (2003)
14. A. Bouferguene et al., Phys. Rev. A **59**, 2712 (1999)
15. W.L. Nighan, Phys. Rev. A **2**, 1989 (1970)
16. M.J.W. Boness et al., Phys. Rev. A **8**, 2883 (1973)
17. C.J. Sweeney, Phys. Rev. A **56**, 1384 (1997)
18. M.A. Morrison, W.G. Sun, *Computational Methods for Electron-Molecule Collisions*, edited by W. Huo, F. Gianturco (Plenum, New York 1995), Chap. 6
19. N.F. Lane, Rev. Mod. Phys. **52**, 29 (1980)
20. M.A. Morrison, Aust. J. Phys. **36**, 239 (1983)
21. M.J. Brennan et al., J. Phys. B: At Mol. Phys. **25**, 2669 (1992)